

Field-Induced Spin-Structural Transition and Giant Magnetostriiction in Ising Chain α -CoV₂O₆

M. Nandi, N. Khan, D. Bhoi, A. Midya, and P. Mandal*

Saha Institute of Nuclear Physics, 1/AF Bidhannagar, Calcutta 700 064, India

E-mail: prabhat.mandal@saha.ac.in

Abstract

We have investigated the temperature and magnetic field dependence of magnetization, specific heat (C_p), and relative sample length change ($\Delta L/L_0$) for understanding the field-induced spin-structural change in quasi-one-dimensional spin chain α -CoV₂O₆ which undergoes antiferromagnetic (AFM) transition below $T_N=15$ K. Analysis of $C_p(T)$ shows that an effective $S=1/2$ Ising state is realized below 20 K, though the magnetic fluctuations persist well above T_N . C_p and the coefficient of linear thermal expansion (α) exhibit strong H dependence in the AFM state. We also observe a huge positive magnetostriiction [$\Delta L(H)/L_0$] below 20 K which does not show any tendency of saturation up to 9 T. With increasing field, a sharp and symmetric peak emerges below T_N in both $C_p(T)$ and $\alpha(T)$ due to field-induced first order ferrimagnetic/ferromagnetic-paramagnetic transitions. The large value of magnetostriiction below T_N suggests strong spin-lattice coupling in α -CoV₂O₆.

KEYWORDS: quasi-one-dimensional, spin chain, antiferromagnetic, ferrimagnetic, field-induced peak in specific heat, thermal expansion, spin-lattice coupling

*To whom correspondence should be addressed

Introduction

Several cobalt-based low-dimensional compounds and rare-earth-based pyrochlore oxides exhibit fascinating magnetic properties such as magnetic field (H) induced spin order-disorder transition,¹ 1/3 magnetization plateau in the $M(H)$ curve,² quantum phase transition³ and spin-structural change.^{4–8} Geometrical frustration due to the triangular or tetrahedral arrangement of the magnetic moments, bond frustration as a result of competing ferromagnetic (FM) and antiferromagnetic (AFM) exchange interactions and large single ion anisotropy are the fundamental ingredients that eventually determine the complexity of the magnetic ground state and hence the new functionalities in these compounds. Often, the ground state of the frustrated materials is extremely sensitive to external perturbations such as magnetic field. Though there are a number of systems showing such kind of magnetic ground state, the underlying mechanism responsible for the above features has not been well understood yet.

Recently, the quasi-one-dimensional (1D) spin-chain CoV_2O_6 has received attention to the scientific community due to the observation of 1/3 magnetization plateau similar to that observed in a regular triangular lattice.^{9–19} In monoclinic $\alpha\text{-CoV}_2\text{O}_6$ and triclinic $\gamma\text{-CoV}_2\text{O}_6$, the edge-shared CoO_6 octahedra form a magnetic chain along the b axis, and the edge-shared VO_5 square pyramids are located in between the magnetic chains. The much larger Co-Co interchain distance as compared to the intrachain Co-Co distance and the presence of the nonmagnetic V^{5+} ion in between the chains weaken the interchain magnetic coupling considerably. Both $\alpha\text{-CoV}_2\text{O}_6$ and $\gamma\text{-CoV}_2\text{O}_6$ show large single ion anisotropy, undergo long-range AFM transition below 15 and 6 K, respectively and exhibit field-induced metamagnetic transitions at two critical fields H_{c1} and H_{c2} .^{9–16} The values of magnetic moment determined from the saturation magnetization (M_S) in the field-induced FM state and susceptibility in the paramagnetic (PM) state are found to be significantly larger than the expected spin-only moment of high spin-state Co^{2+} ion.^{9–11} In $\alpha\text{-CoV}_2\text{O}_6$, M_S is as much as $1.5 \mu_B/\text{Co}$ larger than the spin-only moment ($3.0 \mu_B/\text{Co}$) for H parallel to c axis. This excess $1.5 \mu_B/\text{Co}$ moment is thought to come from the orbital magnetic moment due to the strong

spin-orbit or spin-lattice coupling.^{9–11}

Magnetic, electric, and structural properties have been studied extensively to disclose the underlying mechanism responsible for the step-like jumps in $M(H)$ of CoV_2O_6 .^{9–16} Neutron diffraction studies have revealed that these jumps in $M(H)$ curve are coupled to the field-induced magnetic phase transitions from AFM to FM state through an intermediate ferrimagnetic state.^{13–15} To elucidate the nature of field-induced metamagnetic transition and the thermodynamic properties of frustrated systems, the measurement of specific heat (C_p) in applied field is important. In this work, we present the specific heat data of $\alpha\text{-CoV}_2\text{O}_6$ over a wide range of H across the magnetic ordering at T_N . Strong spin-lattice coupling has also motivated us to investigate the magnetostriction effect $[\Delta L(H)/L_0]$ in this system. We observe that both $C_p(T)$ and the linear thermal expansion coefficient $\alpha(T)$ $[=(1/L_0)d\Delta L(T)/dT]$ exhibit a single λ -like peak at T_N in absence of magnetic field but a sharp and symmetric peak appears below T_N with applied field. Also, the system releases the Ising-like entropy ($R\ln 2$) and exhibits very large magnetostriction effect below $T \sim 20$ K. For understanding the origin of the field-induced magnetic transition in $\alpha\text{-CoV}_2\text{O}_6$, the present results have been compared and contrasted with well known frustrated systems where the field-induced metamagnetic transition occurs due to the triangular or tetrahedral crystal geometry of the magnetic moments.

Experimental details

Polycrystalline $\alpha\text{-CoV}_2\text{O}_6$ samples were prepared by standard solid-state reaction method using high purity cobalt (II) acetate tetrahydrate (Aldrich, 99.999%) and vanadium pentoxide (Alfa Aesar, 99.995%). Stoichiometric quantities of these compounds were mixed properly and the mixture was heated in air for 16 h at 650 °C and then at 725 °C for 48 h. After the heat treatment, the material was quenched in liquid nitrogen to obtain single phase $\alpha\text{-CoV}_2\text{O}_6$. Phase purity was

checked by powder x-ray diffraction (XRD) method with $\text{CuK}\alpha$ radiation in a high resolution Rigaku TTRAX II diffractometer. We have not observed any impurity phase within the resolution ($\sim 2\%$) of XRD. All the peaks in the diffraction pattern were fitted well to a monoclinic structure of space group $C2/m$ using the Rietveld method with an acceptance factor $R_{\text{Bragg}}(\%)=3.78$ (Fig. 1). The observed lattice parameters $a=9.2501 \text{ \AA}$, $b=3.5029 \text{ \AA}$, $c=6.6175 \text{ \AA}$, and $\beta = 111.61^\circ$ are in good agreement with the reported values for $\alpha\text{-CoV}_2\text{O}_6$.¹⁰ We have determined the average grain size ($\sim 35\mu\text{m}$) in the sample using the scanning electron microscope (FEI Quanta 250). The sintered powder was pressed into pellet and then the sample of dimensions $1.5 \times 1.3 \times 1.08 \text{ mm}^3$ was cut from this pellet for the specific heat, magnetostriction and thermal expansion measurements. The longitudinal magnetothermal expansion was measured by capacitive method using a miniature tilted-plates dilatometer with applied field parallel to thickness ($t=1.08 \text{ mm}$) of the sample. The magnetic measurements were done in both physical property measurement system and SQUID-VSM (Quantum Design). The specific heat was measured by conventional relaxation time method using physical property measurement system (Quantum Design).

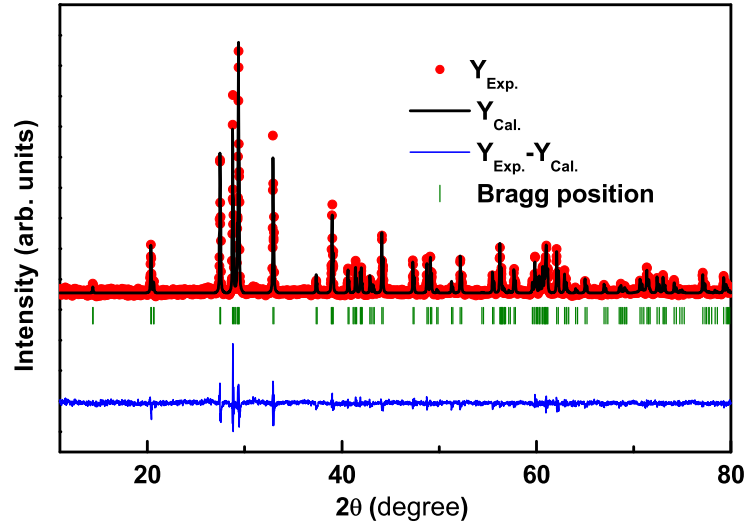


Figure 1: The x-ray powder diffraction pattern for $\alpha\text{-CoV}_2\text{O}_6$ at room temperature. The black solid line corresponds to the Rietveld refinements of the diffraction pattern.

Results and discussion

Figure 2(a) displays the temperature dependence of dc magnetic susceptibility χ ($=M/H$) of polycrystalline α -CoV₂O₆ sample in a field of 0.1 T. χ increases with decreasing T and shows a sharp peak at $T_N=15$ K due to the transition from PM to AFM state. No other peak or anomaly is observed in $\chi(T)$ in the measured temperature range (2-300 K). This indicates that the studied sample does not contain any magnetic impurity. Figure shows that $\chi^{-1}(T)$ can be fitted well to the Curie-Weiss law [$\chi = N\mu_{eff}^2/3k(T - \theta)$] over a wide range of temperature. From this fit, we have calculated the value of effective paramagnetic moment $\mu_{eff}=5.4 \mu_B/\text{Co ion}$ and the Weiss temperature $\theta=-9.2$ K. The negative value of θ implies that the predominant magnetic interaction is antiferromagnetic in nature. The observed value of μ_{eff} is significantly larger than the expected spin-only moment of high spin Co²⁺ ($3.87 \mu_B$). It may be mentioned that Markkula et al. have reported even larger value of μ_{eff} ($6.09 \mu_B/\text{Co}$) for this system.¹³ This huge discrepancy between the observed and expected spin-only moment is due to the strong spin-orbit coupling.⁹⁻¹⁵

The temperature dependence of zero-field specific heat is shown in Fig. 2(b). With decreasing temperature, C_p decreases down to ~ 20 K and then increases rapidly and exhibits a λ -like anomaly close to T_N . Similar to the magnetization data, $C_p(T)$ supports single magnetic phase transition in α -CoV₂O₆. For better understanding the nature of magnetic ground state, the magnetic contribution to the specific heat (C_M) in the vicinity of AFM transition and beyond has been estimated. In the temperature range 50-222 K, C_p can be fitted well with the Einstein model to determine the lattice contribution to the specific heat of the system^{20,21} (please see Figure S1 in the Supporting Information). After subtracting the lattice contribution from C_p , we have plotted C_M in Fig. 2(c). It is clear from Fig. 2(c) that C_M does not decrease rapidly with increasing T in the PM state. The magnetic entropy (S_M) obtained by integrating $(C_M/T)dT$ is also shown in Fig. 2(c). S_M does not saturate even at T as high as $3T_N$, which reflects the highly anisotropic nature of the magnetic structure of α -CoV₂O₆. We would like to mention that the observed value of S_M ($=8.3 \text{ J mol}^{-1} \text{ K}^{-1}$ at $T=3T_N$) for the present sample is about 1.5 times larger than that reported by Kim et al.¹⁸ The larger value of S_M is an indication of superior ordering of spins because it means, more num-

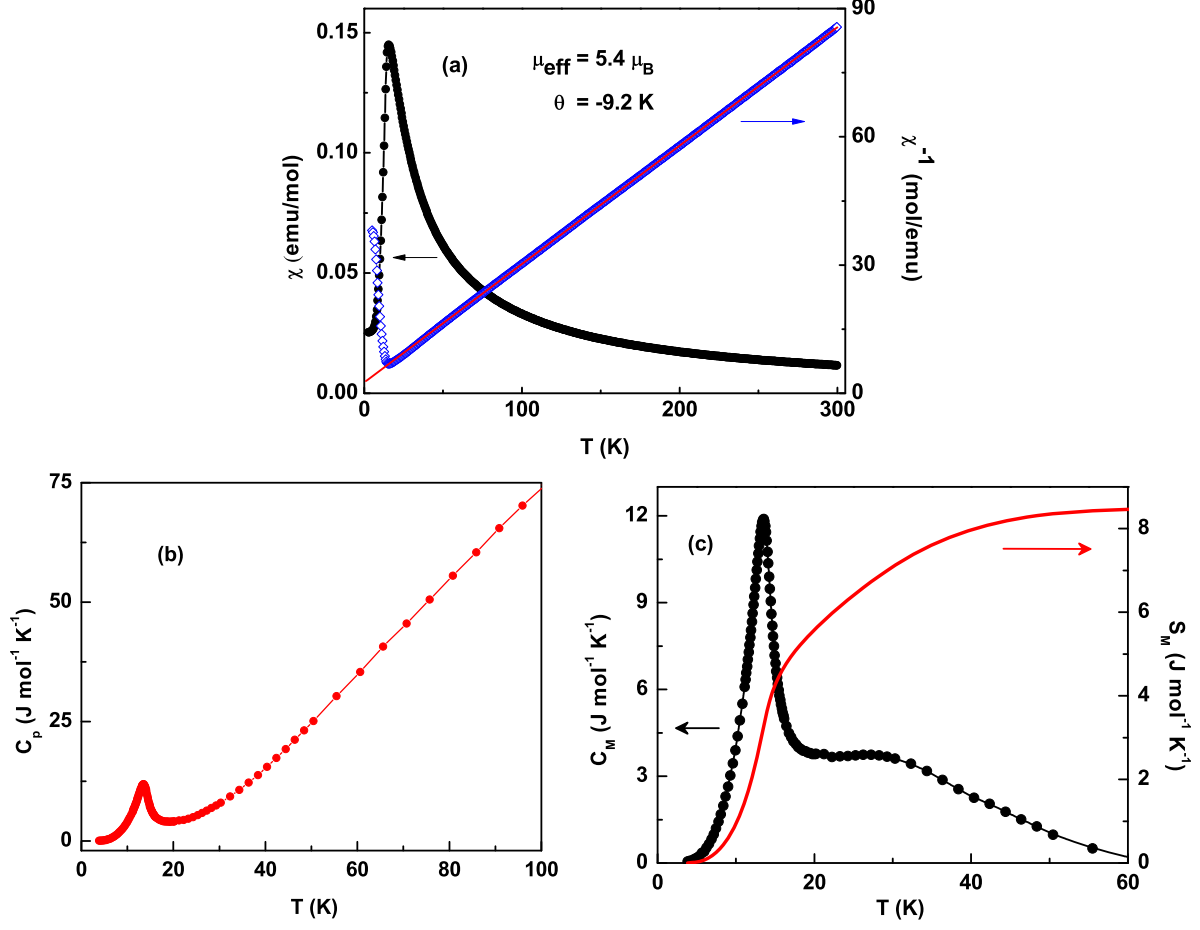


Figure 2: (a) Plots of $\chi(T)$ and $\chi^{-1}(T)$ for α -CoV $_2$ O $_6$ at 0.1 T field. Solid line is the Curie-Weiss fit to the $\chi^{-1}(T)$. (b) The temperature dependence of the specific heat C_p . (c) The temperature dependence of magnetic contribution to the specific heat (C_M) and entropy removal (S_M).

ber of spins are participating in the magnetic transition. The estimated value of S_M , however, is significantly smaller than the expected $11.5 \text{ J mol}^{-1} \text{ K}^{-1}$ for the high spin Co^{2+} ($S=3/2$). It may be noted that $S_M=5.6 \text{ J mol}^{-1} \text{ K}^{-1}$ at 20 K is almost in accord with the expected value ($R\ln 2$) for the degree of freedom of the Ising moments. Thus, the entropy of the Ising-like spins is mostly released below 20 K. As the intrachain ferromagnetic interaction in CoV $_2$ O $_6$ is much stronger than the interchain AFM interaction, the intrachain spin degree of freedom is effectively frozen and the spins would behave like the Ising spins and hence, a huge reduction in magnetic entropy occurs.

Typical specific heat data (C_p/T) in the vicinity of T_N are shown in Fig. 3 as a function of

T for different magnetic fields. The application of magnetic field suppresses and broadens the peak at T_N and the peak position shifts slowly towards lower temperature. Apart from these usual changes, another important feature is emerging with increasing field strength. At a field of 2 T, a weak shoulder-like feature starts to appear in $C_p(T)$ curve just below 11 K. When the applied field exceeds 2 T, this weak anomaly transforms into a sharp and symmetric peak. The sharp nature of the peak suggests that the transition is first-order. As this phenomenon occurs in the neighborhood of strong AFM ordering transition, it is difficult to determine the exact position of the peak. We have determined the positions of the peaks by fitting a pair of Gaussian functions plus a background to the data and found that the peak positions do not shift with field. Also, C_p in the low temperature region is gradually enhanced with increasing field up to 5 T and then decreases. In the antiferromagnetic state, initially magnetic entropy (and hence C_p) increases with H due to the increase of field-induced spin disordering in one of the magnetic sublattices which is antiparallel to applied field. At high fields, however, the volume fraction of FM phase increases significantly and as a result, magnetic entropy reduces. In several AFM systems where field-induced AFM-FM transition occurs, with increasing magnetic field, magnetic entropy initially increases up to a critical field and then decreases.^{22,23}

We now compare the observed specific heat results of α -CoV₂O₆ with that reported for several other frustrated magnetic systems. The two-peak feature in the temperature dependence of the specific heat has been extensively investigated both in theory and experiments.^{5-7,24-27} Several ferrimagnets and quasi-1D AFM spin chains exhibit field-induced peak in C_p due to the opening of an energy gap at low temperature.²⁵⁻²⁷ In these cases, however, the peak is not very sharp and symmetric. Also, the peak shifts and broadens with increasing field strength. In Dy₂Ti₂O₇ pyrochlore, the zero-field $C_p(T)$ exhibits a single peak but a new sharp and symmetric peak appears at very low temperature with the application of magnetic field.^{6,7} We have magnetically aligned the polycrystalline powder sample and done detailed $M(H)$ and $M(T)$ measurements to understand the field and temperature induced transitions. For this aligned sample, $M(H)$ at 5 K and $M(T)$ curves

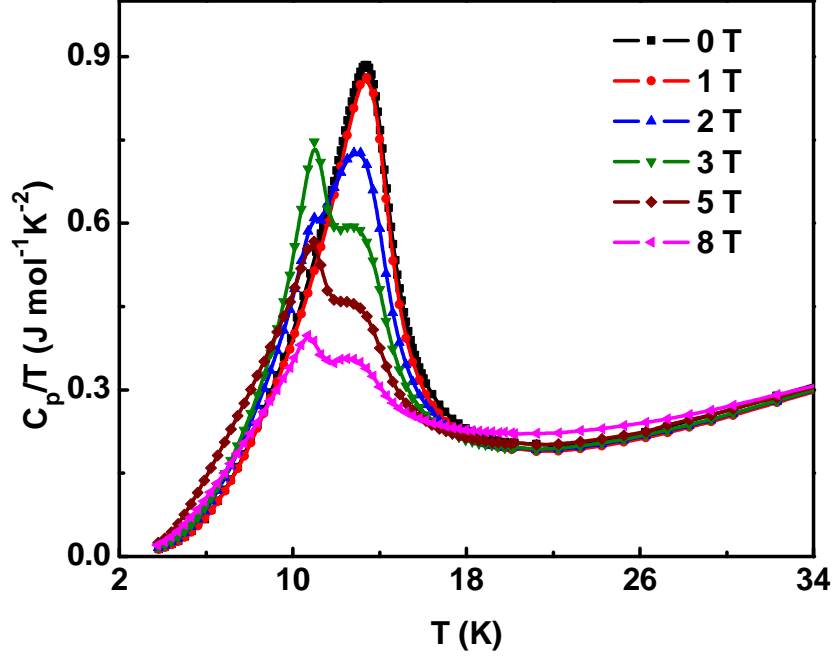


Figure 3: C_p/T versus T plots for α -CoV₂O₆ for different fields in the vicinity of antiferromagnetic transition.

for three different fields are shown in the supporting information section (please see Figures S2 and S3 in the Supporting Information). Similar to randomly oriented powder sample, $M(T)$ shows AFM to PM transition at 15 K for applied field below H_{C1} but $M(T)$ exhibits a sharp peak at 11 K in the field range 1.5-3.3 T due to the transition from ferrimagnetic to PM state. Above 3.3 T where the system is in field-induced FM state, the nature of $M(T)$ curve is very different. With increasing temperature, M decreases very slowly up to about 8 K and then decreases at a faster rate. This behavior of $M(T)$ is typical of a FM system in presence of high magnetic field. Though, the transition region gets smeared, dM/dT reveals a minimum at around 11 K. So it is clear that both ferrimagnetic-PM and FM-PM transitions occur almost at same temperature (11 K). For this reason, we have not observed a third peak in $C_p(T)$ curve at high fields above 3.3 T due to the FM-PM transition. In polycrystalline samples, however, for some crystallites the effective field along the easy axis of magnetization direction can be significantly smaller than the applied field due to their random orientations. Thus, when the applied field exceeds H_{C1} or H_{C2} , these crystallites remain in the AFM or ferrimagnetic state and, as a result, different magnetically ordered phases coexist in the

sample. This observation is fully consistent with the reported low-temperature neutron diffraction results.¹⁵ Powder neutron diffraction studies have revealed the coexistence of different magnetically ordered phases in α -CoV₂O₆ when the strength of applied magnetic field exceeds H_{C1} or H_{C2} .¹⁵ For example, both AFM and ferrimagnetic phases coexist with volume fractions 0.54 and 0.46, respectively at 2.5 T. However, both the phases decrease substantially and FM phase appears at fields above H_{C2} . At 5 T, the volume fractions of AFM, ferrimagnetic and FM phases are 0.20, 0.14 and 0.66, respectively.

In order to shed some more light on the nature and origin of the field-induced peak in C_p , we have studied the linear expansion of sample length $[\Delta L/L]$ as functions of T and H . Figure 4(a) presents $\Delta L(T)/L_{4K}$ ($=[L(T)-L_{4K}]/L_{4K}$) plots up to 45 K for some selected fields, where L_{4K} is the length of the sample at $T=4$ K in an applied field H . The inset of Fig. 4(a) shows $\Delta L(T)/L_{4K}$ plot up to 300 K for $H=0$. At zero field, though $\Delta L/L_{4K}$ decreases monotonically with decreasing T , it starts to decrease at a much faster rate as T approaches T_N . In the PM state, $\Delta L/L_{4K}$ is approximately linear in T below 50 K for field up to 3 T but it develops a broad maximum close to T_N and shows an upward curvature above T_N for higher fields. Though, the anomaly at T_N gets weakened with increasing field strength, it remains visible up to the highest applied field 9 T. At and above 1 T, $\Delta L(T)/L_{4K}$ shows a step-like decrease below a critical temperature $T_S=8$ K. This decrease in $\Delta L/L_{4K}$ at T_S is much sharper in nature than that at T_N . To keep track on the field-evolution of the anomalies at T_N and T_S , we have determined $\alpha(T)$ at different fields from the slope of the curves in Fig. 4(a). Figure 4(b) illustrates the temperature variation of the respective $\alpha(T)$. At zero field, $\alpha(T)$ is positive over the whole temperature range. Similar to $C_p(T)$, $\alpha(T)$ exhibits a sharp λ -like peak close to T_N and the peak shifts to lower temperature and broadens with increasing field. Over a narrow temperature range in the PM state, α becomes small and negative for applied field above 5 T. The field-induced peak in $\alpha(T)$ at T_S is extremely sharp and symmetric and its position is almost insensitive to H . This peak is well separated from AFM transition and visible only below 5 T. In polycrystalline samples, the linear thermal expansion measured using dilatometer is just an

average of the three crystallographic axis directions. Normally, the coefficient of linear thermal expansion measured using dilatometer is 1/3 of the volume expansion coefficient.²⁸ We have compared the present results on thermal expansion with that reported from the temperature variation of lattice parameters determined using powder neutron diffraction.^{13,14} Indeed, the nature of T dependence of the linear thermal expansion is quite similar to the volume expansion determined from powder neutron diffraction data.

The magnetostriction, $\Delta L(H)/L_0 = [L(H) - L_0]/L_0$, where L_0 is the length of the sample in absence

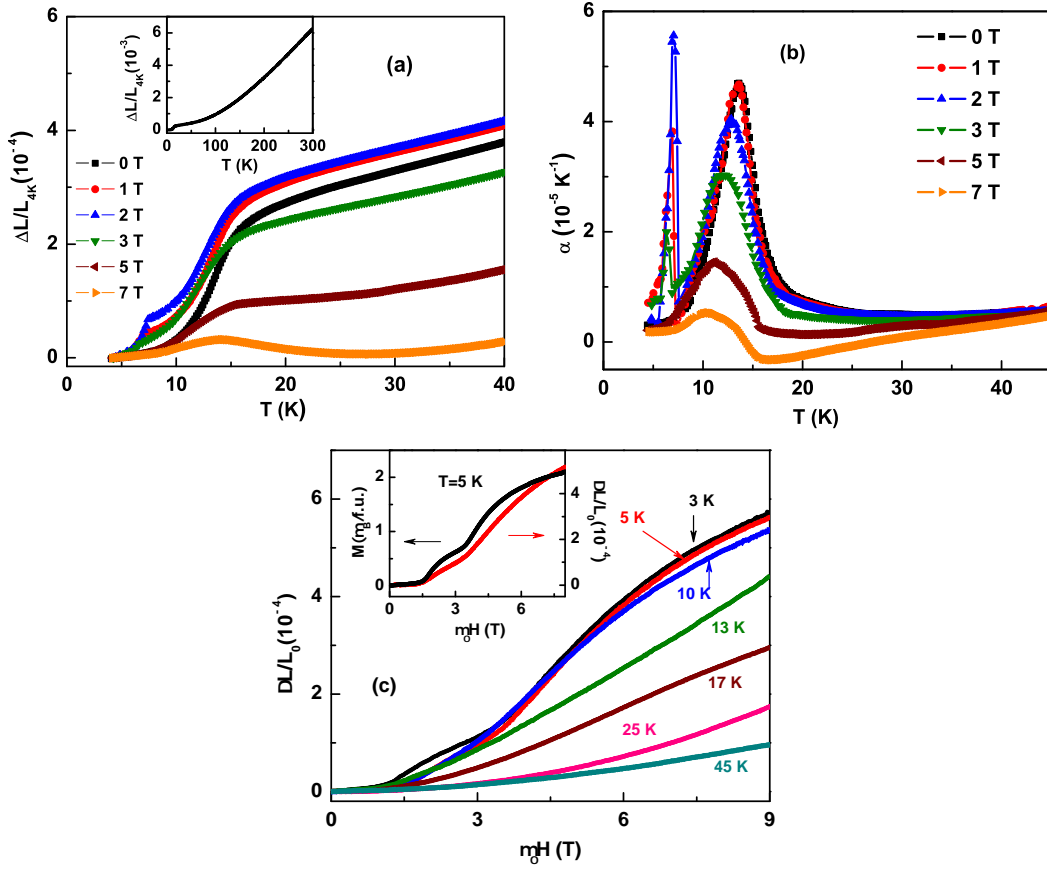


Figure 4: (a) The temperature dependence of the relative length change ($\Delta L/L_{4K}$) for α - CoV_2O_6 for different fields. Inset: $\Delta L(T)/L_{4K}$ in zero field in the temperature range 4-300 K. (b) Plots of the thermal expansion coefficient $\alpha(T)$ for different fields. (c) Magnetostriction, $\Delta L(H)/L_0$, at several temperatures both below and above T_N . Inset: the field dependence of magnetization and $\Delta L/L_0$ at 5 K.

of magnetic field, for some selected temperatures both below and above T_N is depicted in Fig. 4(c). Figure shows that the field dependence of magnetostriction is very sensitive to temperature. At low

temperatures ($T \leq 10$ K), $\Delta L/L_0$ is almost independent of H up to $H_{c1} \sim 1.5$ T. Above H_{c1} , $\Delta L(H)/L_0$ increases rapidly and exhibits a weak anomaly around H_{c2} . Thus, $\Delta L(H)/L_0$ exhibits anomaly at two critical fields that correspond to field-induced metamagnetic transitions in $M(H)$ curve.^{9,10} Similar to $M(H)$, these anomalies are clearly visible at low temperatures but they become weak with increasing T and disappear above $T \simeq 10$ K.^{9,10} The disappearance of these anomalies in both $M(H)$ and $\Delta L(H)/L_0$ curves above 10 K may be related to the observed field-induced first order transition in $C_p(T)$. At low temperature, $\Delta L(H)/L_0$ approximately mimics the nature of $M(H)$ curve [inset of Fig. 4(c)]. $\Delta L(H)/L_0$ develops a downward curvature with the increase of H but it does not show any tendency of saturation up to the maximum applied field. The absence of saturation in $\Delta L(H)/L_0$ is consistent with the nature of $M(H)$ curve. M in single crystals or magnetically aligned sample with field along the c axis saturates above 4 T while M at 7 T is just 50% of the expected value in magnetically random polycrystalline sample.^{9,15} The downward curvature in $\Delta L(H)/L_0$ decreases with increasing T and $\Delta L(H)/L_0$ becomes almost linear for temperatures close to or slightly above T_N . Well above T_N , $\Delta L(H)/L_0$ decreases rapidly with increasing T and develops a weak upward curvature. The magnetostriction effect is very small above 50 K. The unusually high value of the magnetostriction below T_N is comparable to that reported for the frustrated spinels ZnCr_2Se_4 and CdCr_2O_4 where the spin-lattice coupling is believed to be quite strong.^{29,30} In these spinels, however, the nature of H dependence of $\Delta L/L_0$ is different from that for the $\alpha\text{-CoV}_2\text{O}_6$ system. Furthermore, ZnCr_2Se_4 exhibits a strong nearly constant negative thermal expansion over a wide range of T just above T_N which has been attributed to the geometrical frustration of the lattice degrees of freedom.²⁹ In $\alpha\text{-CoV}_2\text{O}_6$, however, $\alpha(T)$ is small and negative only at high fields. The appearance of the peak in $C_p(T)$ and $\alpha(T)$ with applied field and the large positive magnetostriction effect below T_N suggest that the field-induced magnetostructural transition occurs due to the strong spin-lattice coupling and the field-induced FM state occupy more space than the AFM state. We believe that the values of thermal expansion and magnetostriction can be significantly larger in single crystal.

Conclusions

In conclusion, $C_p(T)$ and $\alpha(T)$ of the quasi-1D antiferromagnetic spin chain α -CoV₂O₆ exhibit a sharp λ -like peak around T_N . The magnetic entropy calculated from $C_p(T)$ data shows that the magnetic fluctuations persist well above T_N but the system behaves like a spin-1/2 Ising chain below 20 K. In the AFM state, both C_p and α exhibit strong T and H dependence. When the applied field exceeds H_{c1} , a sharp and symmetric peak emerges well below T_N due to the ferromagnetic/ferrimagnetic-paramagnetic transitions. The sharp nature of the peak indicates that the transition is first order. The huge magnetostriction effect below T_N and its strong H dependence along with the field-induced spin structure transition suggest that the spin-lattice coupling in this system is quite strong. The measurements of C_p and $\Delta L/L$ on single crystal with H along different crystallographic axes may reveal interesting physical properties for α -CoV₂O₆.

Associated Content

Supporting Information

In the temperature range 50-222 K, C_p of α -CoV₂O₆ has been fitted with the Einstein model of lattice specific heat [Figure S1]. The temperature and magnetic field dependence of magnetization have been measured for the magnetically aligned polycrystalline powder sample [Figure S2 and S3]. This material is available free of charge via the Internet at <http://pubs.acs.org>.

References

- (1) He, Z.; Taniyama, T.; K yomen, T.; Itoh, M. Field-Induced Order-Disorder Transition in the Quasi-One-Dimensional Anisotropic Antiferromagnet BaCo₂V₂O₈. *Phys. Rev. B* **2005**, *72*, 172403 1-4.
- (2) Maartense, I.; Yaeger, I.; Wanklyn, B. M. Field-Induced Magnetic Transitions of CoNb₂O₆ in the Ordered State. *Solid State Commun.* **1977**, *21*, 93-96.
- (3) Coldea, R.; Tennant, D. A.; Wheeler, E. M.; Wawrzynska, E.; Prabhakaran, D.; Telling, M.; Habicht, K.; Smeibidl, P.; Kiefer, K. Quantum Criticality in an Ising Chain: Experimental Evidence for Emergent E₈ Symmetry. *Science* **2010**, *327*, 177-180.
- (4) Bramwell, S. T.; Gingras, M. J. P. Spin Ice State in Frustrated Magnetic Pyrochlore Materials. *Science* **2001**, *294*, 1495-1501 and references therein.
- (5) Tabata, Y.; Kadowaki, H.; Matsuhira, K.; Hiroi, Z.; Aso, N.; Ressouche, E.; F  k, B. Kagom   Ice State in the Dipolar Spin Ice Dy₂Ti₂O₇. *Phys. Rev. Lett.* **2006**, *97*, 257205 1-4.
- (6) Ramirez, A. P.; Hayashi, A.; Cava, R. J.; Siddharthan, R.; Shastri, B. S. Zero-Point Entropy in ‘Spin Ice’. *Nature (London)* **1999**, *399*, 333-335.
- (7) Hiroi, Z.; Matsuhira, K.; Takagi, S.; Tayama, T.; Sakakibara, T. Specific Heat of Kagom   Ice in the Pyrochlore Oxide Dy₂Ti₂O₇. *J. Phys. Soc. Jpn.* **2003**, *72*, 411-418.
- (8) Kimura, S.; Takeuchi, T.; Okunishi, K.; Hagiwara, M.; He, Z.; Kindo, K.; Taniyama, T.; Itoh, M. Novel Ordering of an S=1/2 Quasi-1d Ising-Like Antiferromagnet in Magnetic Field. *Phys. Rev. Lett.* **2008**, *100*, 057202 1-4.
- (9) He, Z.; Yamaura, J.; Ueda, Y.; Cheng, W. CoV₂O₆ Single Crystals Grown in a Closed Crucible: Unusual Magnetic Behaviors with Large Anisotropy and 1/3 Magnetization Plateau. *J. Am. Chem. Soc.* **2009**, *131*, 7554-7755.

- (10) Lenertz, M.; Alaria, J.; Stoeffler, D.; Colis, S.; Dinia, A. Magnetic Properties of Low-Dimensional α and γ CoV₂O₆. *J. Phys. Chem. C* **2011**, *115*, 17190-17196.
- (11) Kimber, S. A. J.; Mutka, H.; Chatterji, T.; Hofmann, T.; Henry, P. F.; Bordallo, H. N.; Argyriou, D. N.; Attfield, J. P. Metamagnetism and Soliton Excitations in the Modulated Ferromagnetic Ising Chain CoV₂O₆. *Phys. Rev. B* **2011**, *84*, 104425 1-8.
- (12) Singh, K.; Maignan, A.; Pelloquin, D.; Perez, O.; Simon, Ch. Magnetodielectric Coupling and Magnetization Plateaus in α -CoV₂O₆ Crystals. *J. Mater. Chem.* **2012**, *22*, 6436-6440.
- (13) Markkula, M.; Arevalo-Lopez, A. M.; Attfield, J. P. Neutron Diffraction Study of Monoclinic Brannerite-type CoV₂O₆. *J. Solid State Chem.* **2012**, *192*, 390-393.
- (14) Markkula, M.; Arevalo-Lopez, A. M.; Attfield, J. P. Field-Induced Spin Orders in Monoclinic CoV₂O₆. *Phys. Rev. B* **2012**, *86*, 134401 1-4.
- (15) Lenertz, M.; Alaria, J.; Stoeffler, D.; Colis, S.; Dinia, A. Magnetic Structure of Ground and Field-Induced Ordered States of Low-Dimensional α -CoV₂O₆: Experiment and Theory *Phys. Rev. B* **2012**, *86*, 214428 1-8.
- (16) Lenertz, M.; Colis, S.; Ulhaq-Bouillet, C.; Dinia, A. Epitaxial Growth of γ -CoV₂O₆ Thin Films: Structure, Morphology, and Magnetic Properties. *Appl. Phys. Lett.* **2013**, *102*, 212407 1-4.
- (17) Yao, X. 1/3 Magnetization Plateau Induced by Magnetic Field in Monoclinic CoV₂O₆. *J. Phys. Chem. A* **2012**, *116*, 2278-2282.
- (18) Kim, B.; Kim, B. H.; Kim, K.; Choi, H. C.; Park, S. Y.; Jeong, Y. H.; Min, B. I. Unusual Magnetic Properties Induced by Local Structure in a Quasi-One-Dimensional Ising Chain System: α -CoV₂O₆ *Phys. Rev. B* **2012**, *85*, 220407(R) 1-5.
- (19) Saúl, A.; Vodenicarevic, D. Theoretical Study of the Magnetic Order in α -CoV₂O₆. *Phys. Rev. B* **2013**, *87*, 024403 1-5.

- (20) Hermann, R. P.; Jin, R.; Schweika, W.; Grandjean, F.; Mandrus, D.; Sales, B. C.; Long, G. J. Einstein Oscillators in Thallium Filled Antimony Skutterudites. *Phys. Rev. Lett.* **2003**, *90*, 135505 1-4.
- (21) Long, Y.; Liu, Q.; Lv, Y.; Yu, R.; Jin, C. Various $3d-4f$ Spin Interactions and Field-Induced Metamagnetism in the Cr^{5+} System DyCrO_4 . *Phys. Rev. B* **2011**, *83*, 024416 1-6.
- (22) Midya, A.; Mandal, P.; Das, S.; Banerjee, S.; Sharath Chandra, L. S.; Ganesan, V.; Roy Barman, S. Magnetocaloric Effect in HoMnO_3 Crystal. *Appl. Phys. Lett.* **2010**, *96*, 142514 1-4.
- (23) Midya, A.; Das, S. N.; Mandal, P.; Pandya, S.; Ganesan, V. Anisotropic Magnetic Properties and Giant Magnetocaloric Effect in Antiferromagnetic RMnO_3 Crystals ($R=\text{Dy}$, Tb , Ho , and Yb). *Phys. Rev. B* **2010**, *84*, 235127 1-10.
- (24) Antonosyan, D.; Bellucci, S.; Ohanyan, V. Exactly Solvable Ising-Heisenberg Chain with Triangular XXZ-Heisenberg Plaquettes. *Phys. Rev. B* **2009**, *79*, 014432 1-11.
- (25) Li, W.; Gong, S. S.; Zhao, Y.; Ran, S. J.; Gao, S.; Su, G. Phase Transitions and Thermodynamics of the Two-Dimensional Ising Model on a Distorted Kagome Lattice. *Phys. Rev. B* **2010**, *82*, 134434 1-8.
- (26) Honda, Z.; Katsumata, K.; Yamada, K. The Spin Gap in a Quantum Antiferromagnet on the Kagomé Lattice. *J. Phys.: Condens. Matter* **2002**, *14*, L625-629.
- (27) Yoshida, Y.; Tateiwa, N.; Mito, M.; Kawae, T.; Takeda, K.; Hosokoshi, Y.; Inoue, K. Specific Heat Study of an $S = 1/2$ Alternating Heisenberg Chain System: F_5PNN in a Magnetic Field. *Phys. Rev. Lett.* **2005**, *94*, 037203 1-4.
- (28) Souza, J. A.; Neumeier, J. J.; White, B.D.; Yu, Yi-Kou. Analysis of the Critical Behavior Associated with the Antiferromagnetic Transitions of LaMnO_3 and CaMnO_3 . *Phys. Rev. B* **2010**, *81*, 172410 1-4.

- (29) Hemberger, J.; Krug von Nidda, H.-A.; Tsurkan, V.; Loidl, A. Large Magnetostriction and Negative Thermal Expansion in the Frustrated Antiferromagnet ZnCr_2Se_4 . *Phys. Rev. Lett.* **2007**, 98, 147203 1-4.
- (30) Ueda, H.; Katori, H. A.; Mitamura, H.; Goto, T.; Takagi, H. Magnetic-Field Induced Transition to the 1/2 Magnetization Plateau State in the Geometrically Frustrated Magnet CdCr_2O_4 . *Phys. Rev. Lett.* **2005**, 94, 047202 1-4.

Supporting Information

The temperature dependence total specific heat (C_p) is shown in Fig. S1. In the range 50-222 K, C_p is fitted well by the Einstein model of lattice specific heat. In order to extract the lattice contribution to C_p in the paramagnetic (PM) as well as in the antiferromagnetic (AFM) states, the Einstein fitting curve has been extrapolated down to lowest measured temperature (2 K).

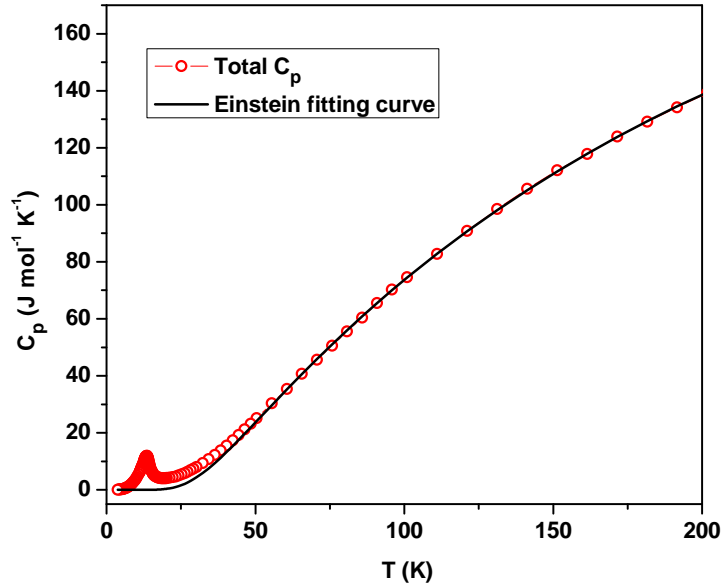


Figure S1: The fitting of the specific heat (C_p) data with the Einstein model of lattice specific heat. The black line represents the Einstein fitting curve and the red symbol represents the total specific heat.

We have aligned the powder sample of α - CoV_2O_6 in a polymeric glue by applying 7 T magnetic field at room temperature which freezes the particle orientation. The field dependence of magnetization (M) at 5 K is shown in Fig. S2. It is clear from the figure that $M(H)$ exhibits sharp field-induced transitions at two critical fields (H_{c1} and H_{c2}) and 1/3 magnetization plateau between H_{c1} and H_{c2} , and the saturation value of M in the ferromagnetic (FM) state (above H_{c2}) is about $4.6 \mu_B/\text{Co}$.

Figure S3 shows representative $M(T)$ curves at three different magnetic fields of aligned polycrystalline α - CoV_2O_6 . At 0.1 T, an AFM-PM transition occurs around 15 K (upper panel). For

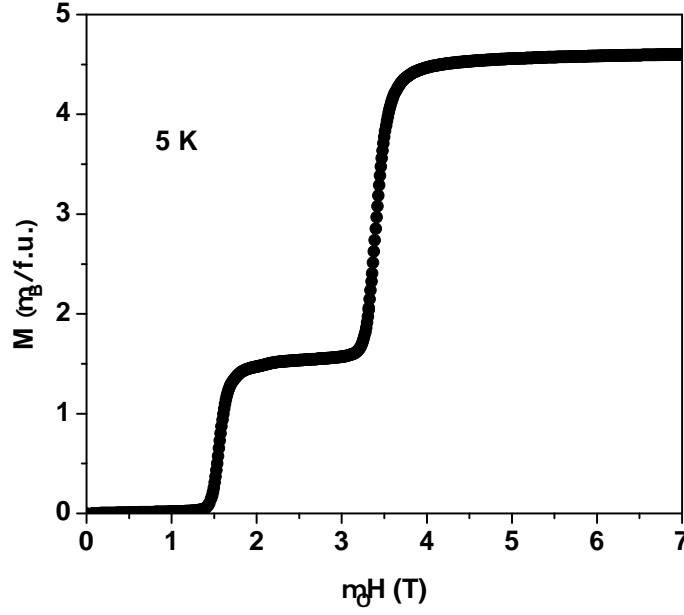


Figure S2: The field dependence of magnetization of aligned α -CoV₂O₆ sample at 5 K.

$H_{c1} < H < H_{c2}$, the peak due to AFM-PM transition disappears but a new peak appears at lower temperature (11 K) due to ferrimagnetic-PM transition (middle panel). However, above H_{c2} , the nature of $M(T)$ curve is typical of a FM system in high field with FM-PM transition ~ 11 K (lower panel). This study shows that α -CoV₂O₆ undergoes ferrimagnetic-PM and FM-PM transitions at same temperature (11 K).

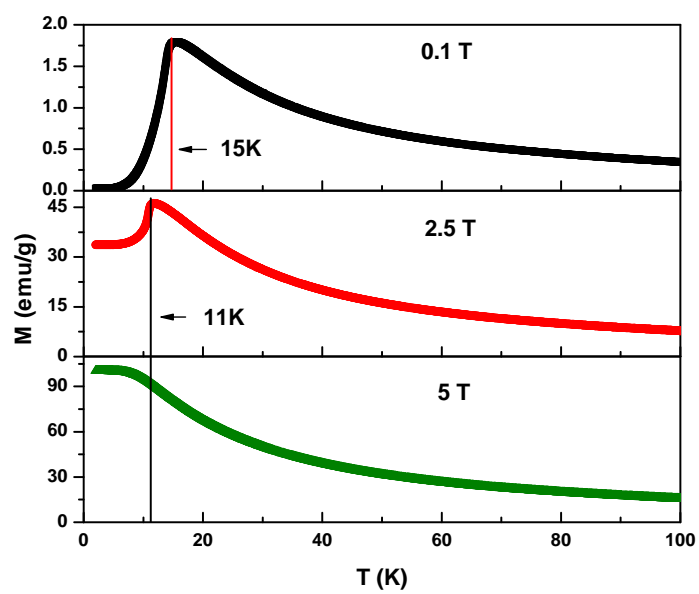


Figure S3: Three representative $M(T)$ curves for the magnetically aligned α - CoV_2O_6 sample.